Jang and Kang *Int J Concr Struct Mater* (2019) 13:29
https://doi.org/10.1186/s40069-019-0341-4

International Journal of Concrete Structures and Materials

RESEARCH Open Access

Punching Shear Behavior of Shear Reinforced Slab–Column Connection with Varying Flexural Reinforcement

Jae-Ick Jang and Su-Min Kang*

Abstract

The effects of flexural reinforcement and shear reinforcement on the punching shear strength of slab–column connections are analyzed in this study. For the study, six slab–column connection specimens were constructed with varying flexural reinforcement and shear reinforcement, and were subjected to gravity load tests. Experimental results showed that all specimens were destroyed by punching failure, and that the slab–column connection behaved differently depending on the amount of shear reinforcement and flexural reinforcement. Particularly, the flexural reinforcement in the slab–column connection improved the punching strength of the specimens with or without shear reinforcement. In addition, in this study, a design formula that considers the flexural reinforcement ratio in the calculation of the punching shear strength of the shear reinforced slab–column connection was proposed and was verified using experimental results and existing test data.

Keywords: shear reinforcement, flexural reinforcement, slab, column, punching shear, stirrup

1 Introduction

Flat plate structures consisting of slabs and columns are widely used in apartment houses, offices, and skyscrapers due to their architectural and construction advantages. However, relatively thin slabs in the flat plate system are vulnerable to punching shear failure at the slab–column connection; punching shear failure is more dangerous than other ductile failure modes such as flexural failure, as punching shear failure is sudden and may induce collapse of the entire system (Choi and Park 2010; Choi et al. 2011, 2012). Therefore, in current concrete design codes such as ACI 318 (ACI 2014) and KCI 2012 (KCI 2012), shear reinforcement is adopted to ensure the sufficient strength against punching shear at the slab–column connection.

A recent study on the shear reinforcement of slab–column connections proposed that the time at which the maximum punching strength of the slab–column connection occurs varies depending on the amount of shear reinforcement. According to the study conducted by Eom et al. (2018), slab–column connections with low shear reinforcement exhibit ultimate punching shear strength at the initial diagonal crack state of concrete. This is because the shear reinforcement is insufficient to recover the shear strength reduction of the concrete after the initial diagonal crack of the concrete. However, when the shear reinforcement is sufficient, it recovers the shear strength reduction of the concrete after the initial diagonal crack; hence, the ultimate strength occurs after the initial diagonal crack. Therefore, in the study by Eom et al. (2018), a formula to evaluate the punching shear strength (Eq. 1) was proposed as given below, based on the difference of the time of maximum strength occurrence with varying shear reinforcement and the difference of contribution of the concrete and shear reinforcement.

$$V_{n,Eom's} = \max(V_c + 0.25V_s, 0.5V_c + V_s) \tag{1}$$

where, V_c is the shear strength of the concrete, V_s is the shear strength of the shear reinforcement.

*Correspondence: kangsm@cbnu.ac.kr
Department of Architectural Engineering, Chungbuk National University, 1 Chungdae-ro, Seowon-Gu, Cheongju, Chungbuk 361-763, South Korea
Journal information: ISSN 1976-0485 / eISSN 2234-1315

However, the current concrete design codes (ACI 2014; KCI 2012) do not consider the difference in the behavior of slab-to-column connections with varying shear reinforcement. They evaluate the punching shear strength by reducing the contribution of the concrete and shear reinforcement according to the design philosophy of each code. Equations (2) and (3) are used to evaluate the punching shear strength for ACI 318 (ACI 2014) and KCI 2012 (KCI 2012), respectively.

$$V_{n,ACI} = 0.5V_c + V_s \quad (2)$$

$$V_{n,KCI} = V_c + 0.5V_s \quad (3)$$

where, V_c is the shear strength of the concrete, V_s is the shear strength of the shear reinforcement.

As shown in Eq. (2), in the case of ACI 318 (ACI 2014), the punching shear strength of the shear reinforced connection is calculated by reducing the concrete strength by 50%, which is similar to the punching shear evaluation for connections with sufficient shear reinforcement in a previous study (Eom et al. 2018). On the other hand, as shown in Eq. (3), in the case of KCI 2012 (KCI 2012), the punching shear strength of the shear reinforced connection is calculated by reducing the contribution of the shear reinforcement by 50% assuming that the shear reinforcement does not yield like the connection with low shear reinforcement in the study by Eom et al. (2018). However, it is necessary to closely examine whether the latest research results such as those of Eom at al. (2018) lead to valid results in various design conditions (Choi and Song 2007; Choi et al. 2005).

ACI 318 (ACI 2014) also evaluates the punching shear strength contribution by concrete as shown in Eq. (4). In Eq. (4), the punching shear strength contribution by concrete is evaluated considering only the concrete strength and connection shape regardless of the flexural reinforcement.

$$V_{c,ACI} = \frac{1}{6}\sqrt{f_{kc}}b_0 d \times min\left(1 + \frac{2}{\beta_c}, 1 + \frac{\alpha_s d}{b_0}, 2\right) \quad (4)$$

where, f_{ck} is the compressive strength of the concrete, d is the effective thickness of the slab, b_o is length of the critical shear perimeter at a distance 0.5d from the column face, β_c is the ratio of the long side to the short side of the area subjected to concentrated load or reaction force, α_s is a factor according to the type of connection; it is 40 for internal columns, 30 for external columns (except corner columns), and 20 for corner columns.

On the other hand, unlike ACI 318 (ACI 2014), KCI 2012 (KCI 2012) evaluates the punching shear strength contribution by concrete considering the effect of flexural reinforcement ratio on the punching shear strength as shown below.

$$V_{c,KCI} = v_{c,KCI} b_0 d \quad (5)$$

$$v_{c,KCI} = k_s k_{bo} f_{te} cot\psi (c_u/d) \quad (6)$$

$$c_u = d\left[25\sqrt{\rho/f_{ck}} - 300\left(\rho/f_{ck}\right)\right] \quad (7)$$

where, $k_s = \sqrt[4]{300/d} \le 1$, $k_{bo} = 4/\sqrt{b_0/d} \le 1.25$, $f_{te} = 0.21\sqrt{f_{ck}}$, $f_{cc} = (2/3)f_{ck}$, $\cot\psi = \sqrt{f_{te}\left(f_{te} + f_{cc}\right)}/f_{te}$, k_s is the thickness factor, k_{bo} is the effect factor of the critical section length, f_{te} is the tensile strength of the compression zone in concrete, c_u is the average depth of the compression zone in concrete, f_{cc} is the compressive strength of the compression zone in concrete, ψ is the crack angle of the compression zone in concrete.

In the Eq. (7), which is for KCI 2012 (KCI 2012), the effect of the flexural reinforcement ratio is included. It is known that KCI 2012 (KCI 2012) estimates the punching shear strength by concrete more accurately (Choi and Park 2010), compared with ACI 318 (ACI 2014), because the effect of flexural reinforcement is considered in the KCI 2012 code (KCI 2012).

However, in ACI 318 (ACI 2014) and KCI 2012 (KCI 2012), when the punching shear strength by shear reinforcement is calculated as shown in Eq. (8), the effect of the flexural reinforcement is not considered.

$$V_S = \frac{A_s f_y d}{s} \quad (8)$$

where, A_s is the sectional area of shear reinforcement, f_y is the yield strength of shear reinforcement, s is the spacing of shear reinforcement.

As flexural reinforcement affected the punching shear strength by the contribution of the concrete, it is also necessary to examine the interaction of flexural and shear reinforcement on the punching strength. Therefore, in this study, the effect of flexural reinforcement on the ultimate behavior of slab–column connections was studied comprehensively through experimental work. Particularly, the effect of flexural reinforcement on the punching shear strength of the shear reinforcement was examined. Further, the recent research findings by Eom et al. (2018) were verified using various amounts of flexural reinforcements. The current design codes such as ACI 318 (ACI 2014) and KCI 2012 (KCI 2012) were analyzed for the effects of various flexural reinforcement ratios, in order to verify if the punching strength of the slab–column connection is effectively reflected in these codes. Finally, a design formula that considers the flexural reinforcement ratio to calculate the punching shear strength of the shear reinforced slab–column connection was proposed and verified using experimental results and existing test data.

2 Test Plan

In this study, six slab–column connection specimens (SP 1–6) were constructed with varying flexural reinforcement and shear reinforcement. All specimens were designed to induce punching shear failure in accordance with the purpose of the experiment. The amounts of flexural reinforcement and shear reinforcement were used as test variables. The experimental variables for SP-1–6 are shown in Table 1.

Figure 1 shows a three-dimensional model of all the slab–column connection specimens. As shown in Fig. 1, the specimens contain a slab of dimensions 1850 mm (width) × 1850 mm (length) × 210 mm (thickness) and a column of dimensions 450 mm (width) × 450 mm (length) × 200 mm (height).

Figure 2a shows the test set-up. For convenience, the specimen shown in Fig. 1 was turned upside down and load was applied from the bottom of the specimen. As shown in Fig. 2, the specimen was supported by a simple support at each side of the slab, and the test was carried out by applying a load to the upper column. The vertical displacement of the slab–column connection was measured by LVDTs (The linear variable differential transformer) which are shown in Fig. 2b.

Figure 3a–f shows the specimen details of the slab–column connection (SP-1–6), whose properties are summarized in Table 1. As shown in Table 1, the test variables of specimens SP-1–6 were the amounts of flexural reinforcement and shear reinforcement. For specimens SP-1–3, the flexural reinforcements were placed with D16@150 at the top surface of the slab. The specimens' flexural reinforcement ratio was 0.007, with low flexural reinforcement among the six specimens. For SP-4–6, the flexural reinforcements were placed with D16@75 at the top of the slab, and were twice the flexural reinforcement of the SP-1–3 specimens. The specimens' flexural reinforcement ratio was 0.014, with high flexural reinforcement among the six specimens.

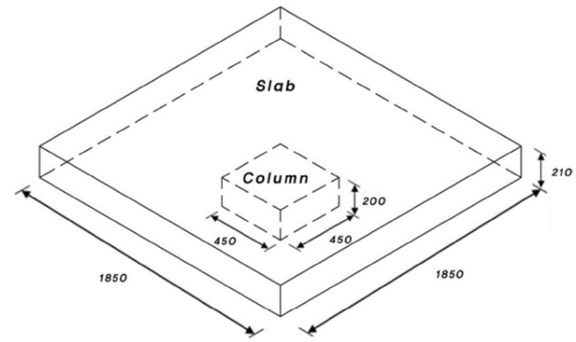

Fig. 1 Configuration of slab–column connection specimen.

By varying the amount of shear reinforcement the specimens with the same flexural reinforcement (SP 1–3 and SP 4–6), a total of six specimens were prepared. Among the specimens with low flexural reinforcement ratio (SP-1–3), SP-1 was not reinforced by shear reinforcement, and was a control specimen to verify whether the original design concept had been properly implemented. SP-2 had a small amount of shear reinforcement. Two rows of D10 single-leg stirrups were placed at a spacing of 85 mm as a shear reinforcement along both principal directions. SP-3 had a large amount of shear reinforcement. Four rows of D10 single-leg stirrups were placed at a spacing of 85 mm as a shear reinforcement along both principal directions. SP-3 had twice the amount of shear reinforcement than SP-2. Therefore, the objective was to investigate the behavior of the slab–column connections with varying shear reinforcement.

Specimens with high flexural reinforcement ratio (SP-4–6) were designed to investigate the behavior of the slab–column connections with varying flexural reinforcement, and compared with specimens with low flexural reinforcement ratio (SP-1–3). The aim was to investigate the effect of the flexural reinforcement on the punching shear strength and the behavior of shear reinforcement

Table 1 Summary of test specimens.

Specimens	d (mm)	Flexural reinforcement		Shear reinforcement
		Top bar (ρ)	Bottom bar (ρ)	Type and spacing (for each direction)
SP-1	174	D16@150 in two direction (0.007)	D10@130 in two direction (0.003)	N/A
SP-2				2-D10@85
SP-3				4-D10@85
SP-4		D16@75 in two direction (0.014)	D16@150 in two direction (0.007)	N/A
SP-5				2-D10@85
SP-6				4-D10@85

Nominal diameter of D10 is 9.53 mm

Nominal diameter of D16 is 15.9 mm

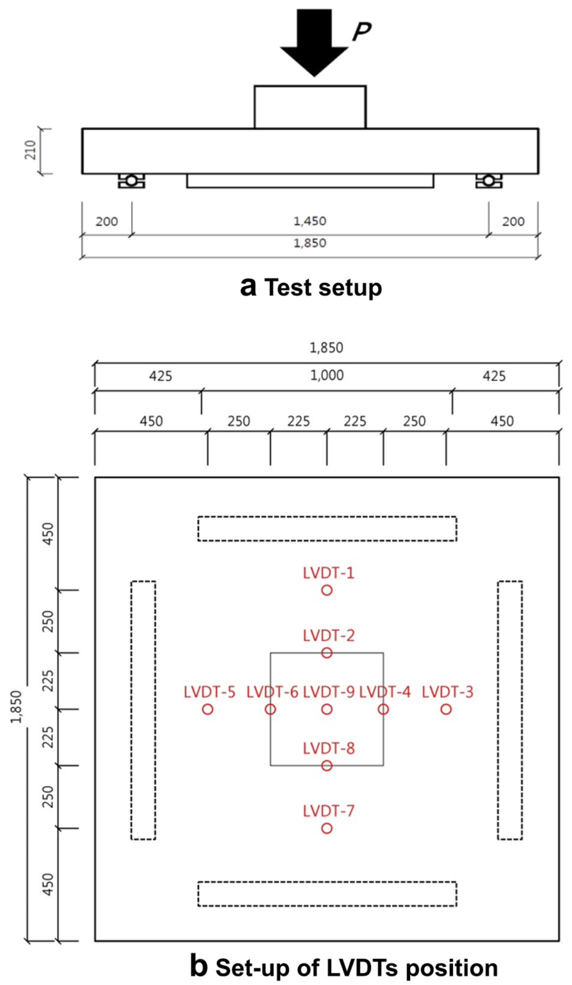

Fig. 2 Test setup for punching shear test. **a** Test set-up, **b** Location of LVDTs.

with varying flexural reinforcement. Therefore, except for the flexural reinforcement, the details and design concepts of SP-4–6 were the same as those of SP-1–3. The shear reinforcement of specimens SP-4–6 was equal to that of SP-1–3.

3 Test Results

3.1 Result of Material Test

Specimen construction and loading were carried out twice, on SP-1–3 and SP-4–6, based on the amount of flexural reinforcement. Material tests were performed to investigate the concrete compressive strength and tensile strength of the reinforcement. Material tests were performed on the same day as for the test of the slab–column connections. The result of the material test, in term of the concrete compressive strength and yield strength of the reinforcement, are shown in Tables 2 and 3, respectively. The compressive strength of concrete was larger than the expected 30 MPa in the initial design; it was measured as 34 MPa in SP-1–3 and 44 MPa in SP-4–6. The yield strengths of reinforcing bars D10 (400 MPa) and D16 (600 MPa) were 513 MPa and 652 MPa for SP-1–3 and 459 MPa and 635 MPa for SP-4–6, respectively. In this study, the design yield strength of flexural reinforcing bars D16 was planned to be higher than that of shear reinforcing bars D10 to induce punching shear failure rather than flexural yielding of the slabs.

3.2 Load–Deflection Relationship

Figure 4 shows the load–deflection relationship of the SP-1–6, slab–column connection specimens. The central displacement of the specimen, which is the X-axis value, was measured using the LVDT 9 (Fig. 2b), and the load on the Y-axis was the load applied in the direction of gravity in Fig. 2a. Table 4 summarizes the maximum load and central deflection at the maximum load of specimens SP-1–6 in Fig. 4. Figure 4a shows the load–deflection relationship for SP-1–3 with a small amount of flexural reinforcement, and Fig. 4b shows the load–deflection relationship for SP-4–6 with a large amount of flexural reinforcement. In order to compare the effect of the amount of flexural reinforcement on the strength of the slab–column connections, the load–deflection relations in Fig. 4a, b for SP-1–6 are collectively shown in Fig. 4c.

Figure 4a is a load–deflection graph of SP-1–3 with a small amount of flexural reinforcement. Table 4 shows the ultimate strength and central displacement at the initial diagonal crack. SP-1–3 have similar vertical displacements at the ultimate strength. The strength of the specimen without shear reinforcement was 776 kN (SP-1), whereas that with shear reinforcement was 1029 kN (SP-2) and 970 kN (SP-3). Although SP-3 has twice the amount of shear reinforcement compared to SP-2, the ultimate punching strengths of SP-2 and SP-3 were not significantly different. Rather, the strength of SP-2, which has a smaller amount of shear reinforcement, was measured to be higher than that of SP-3. In general, shear reinforcement is added to increase the shear strength of slab–column connections. However, experimental results indicate that for slab–column connections with a small amount of flexural reinforcement, the punching shear strength does not increase sufficiently even if more shear reinforcement is added. However, the graph for SP-3 is different from that of SP-2. At the ultimate strength, SP-3 has a smaller vertical displacement than SP-2 and was destroyed at low load; however, SP-3 shows better ductility than SP-2. These results show that after the ultimate strength, shear reinforcement affects the ductile behavior of the slab–column connections.

Figure 4b shows the load–deflection graph of SP-4–6 with a large amount of flexural reinforcement. For

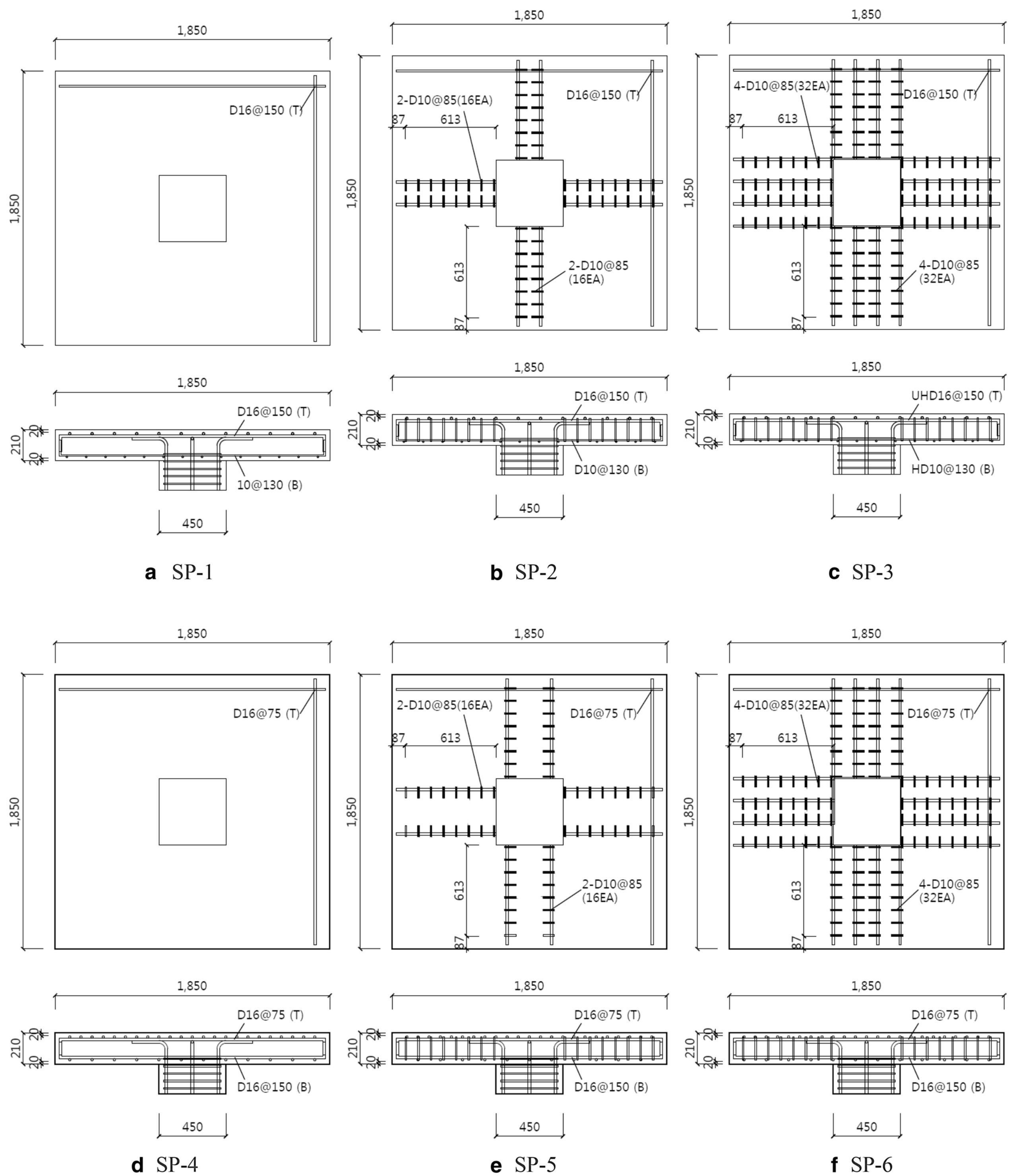

Fig. 3 Reinforcement details of test specimens.

SP-4–6, unlike SP-1–3 in Fig. 4a, the ultimate strength increased in the order of SP-4–6 as the shear reinforcement increased, and the displacement at maximum load also increased. For SP-6, which had a large amount of shear reinforcement, unlike the other specimens, the shear strength after the initial diagonal cracks was higher

Table 2 Concrete compressive strength test.

Specimens	Strength (MPa)	Average strength (MPa)
SP-1–3	32.84	34
	29.49	
	39.5	
SP-4–6	43.82	44
	43.62	
	44.44	

Table 3 Rebar tensile strength test.

Specimens	type	Strength (MPa)	Average strength (MPa)
SP-1–3	D10	508	513
		538	
		495	
	D16	650	652
		654	
		652	
SP-4–6	D10	480.22	459
		427.05	
		468.06	
	D16	610	635
		667.42	
		628.39	

than that at the initial diagonal crack due to an increase in ductility after the initial diagonal crack. For a large amount of flexural reinforcement, these results are consistent with those reported by Eom et al. (2018).

In Fig. 4c, all the graphs of SP-1–6 were compared with varying flexural reinforcement and shear reinforcement. Figure 4c shows that the stiffness of the specimens before the ultimate strength varies depending on the difference in the flexural reinforcement ratio. SP-4–6 with a high flexural reinforcement ratio show larger stiffness than SP-1–3 with a low flexural reinforcement ratio.

In SP-4–6 where the flexural reinforcement was large, the strength of SP-6 increased after the initial diagonal cracking. The initial diagonal cracks in the concrete are considered to have occurred at the point of the first peak in the load displacement graph of the test specimen. According to previous study (Eom et al. 2018), at the first peak, two-way concrete cracking began to occur significantly and the contribution of shear reinforcements to the slab punching shear strength was less than 50% of their yield strength. However, in SP-1–3, where the flexural reinforcement was small, an increase in strength after the initial diagonal cracking was not observed. In SP-3, which had the same amount of shear reinforcement as SP-6 which showed an increase in strength, no additional strength increase was observed. SP-3 and SP-6 behave differently depending on the amount of flexural reinforcement, indicating that the results of Eom et al. (2018) can be effective in limited conditions. Eom et al. (2018) reported that if the amount of shear reinforcement is increased regardless of the amount of flexural reinforcement, the ultimate punching strength increases after the initial diagonal crack, as shown in the graph for SP-6. However, in this study, the behavior of SP-3, which had a small amount of flexural reinforcement, was different. Therefore, only the amount of shear reinforcement does not determine this strength increase after initial diagonal cracking. Moreover, the flexural reinforcement should be more than a certain amount for this strength increase after initial diagonal cracking.

In general, if the punching shear strength is insufficient in the design of slab–column connections, it could be made sufficient by adding shear reinforcement. However, adding shear reinforcement with hook detail on a thin slab significantly degrades the constructability. Figure 4c shows that the punching shear strength increases even more when only the flexural reinforcement is added to the control specimen (SP-1), such as the case of SP-4, than when the shear reinforcement is added to the control specimen (SP-1), such as the case of SP-2 or SP-3. Hence, if the punching shear strength is to be increased at the slab–column connection, additional flexural reinforcement could only be provided to the slab region where the slab–column is located, instead of shear reinforcement. Furthermore, additional reinforcement in the form of flexural reinforcement in a limited region will have a positive effect on constructability, as it replaces the complex set-up for shear reinforcement.

3.3 Crack and Failure Mode

Figure 5 shows the cracks and failure pattern on the opposite side of the column immediately after the end of the experiment for SP-1–6. All specimens show similar shear cracks, with pierced shear failure and a similar cross section. However, on comparing the amounts of flexural reinforcements, SP-2–3 with a low flexural reinforcement ratio exhibit a distinct failure surface than SP-5–6 with a high flexural reinforcement ratio. In addition, SP-4–6 with a high flexural reinforcement ratio appear to have more small distributed cracks than SP-1–3 with a low flexural reinforcement ratio. For SP-2 and SP-5 with the same small amount of shear reinforcement, the hook for shear reinforcement was spread by the applied punching load, and the concrete cover was burst out. On the other hand, for SP-3 and SP-6 with the

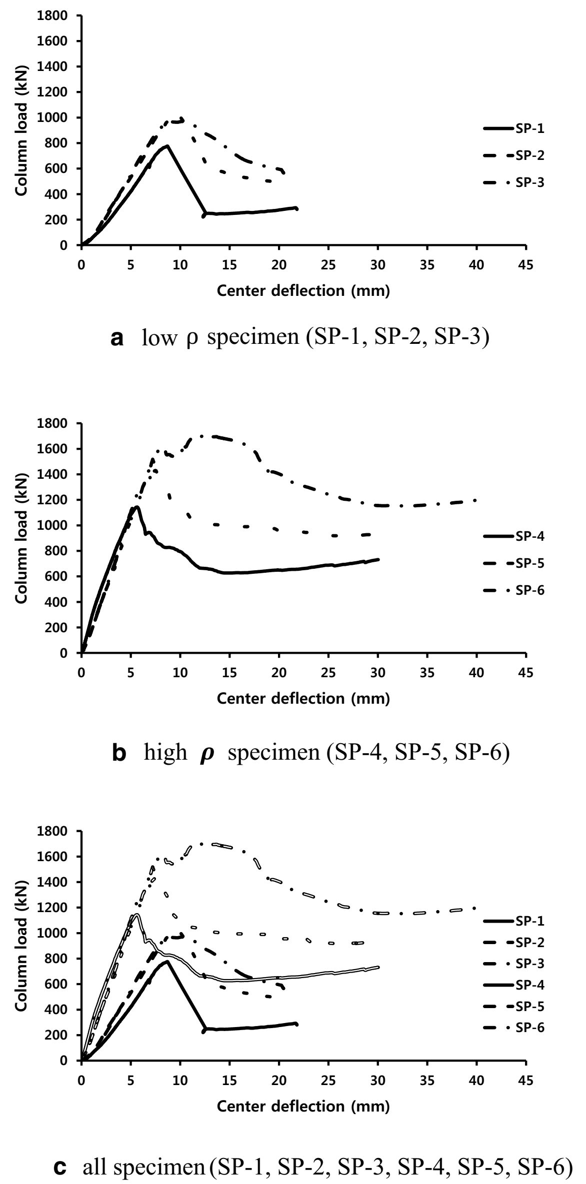

Fig. 4 Vertical load–center deflection relationships of test specimens.

Table 4 Maximum load and center deflection of test specimens.

Specimens	Maximum load (kN)	Center deflection at maximum load (mm)
SP-1	776	8.68
SP-2	1029	9.72
SP-3	970	8.88
SP-4	1143	5.61
SP-5	1429	7.46
SP-6	1713	12.82

same sufficient amount of shear reinforcement, this phenomenon did not occur; instead typical punching shear failure occurred. For SP-3 and SP-6 with a higher shear reinforcement, the load applied to each shear reinforcement is reduced, the hook of the shear reinforcement can maintain its shape, and the concrete does not burst out to the maximum load.

3.4 Strain of Reinforcement

Figure 6 shows the location and number of strain gauges installed on the flexural reinforcement and shear reinforcement of SP-1–6. In Fig. 6a, d, the strain gauges for flexural reinforcement were installed at the same positions in two groups, SP-1–3 and SP-4–6. The strain gauges of Fig. 6a, d for flexural reinforcement were installed at the column surface of the specimen where the bending moment might be maximum, and between the column surface and supporting points. Strain gauges for shear reinforcement at shear reinforced specimens SP-2, 3, 5, and 6 were installed at positions shown in Fig. 6b, c, e and f, respectively. In Fig. 6b, c, e and f, strain gauges for shear reinforcement were installed on the basis of the expected critical section of the specimen. Figure 7 shows the load–displacement graph of Fig. 4 and the strains of the re-bars from gauges which were installed at the locations shown in Fig. 6 for each specimen to easily understand the behavior of the rebar under the ultimate state. In Fig. 7, the X-axis of the graph is the displacement of LVDT-9, which is the vertical displacement at the center of the connection. The Y axis is the ratio of the strain of the rebar (ε_s) to the yield strain of the rebar (ε_y), and it is judged that the rebar yielded when $\varepsilon_s/\varepsilon_y = 1$. The red dashed line in Fig. 7 shows the initial diagonal crack strength and the corresponding displacement of the specimen. The blue dashed line shows the initial diagonal crack strength and the corresponding displacement of the SP-1 and SP-4, which were compared with other specimens possessing the same flexural reinforcement ratio in the load–displacement graph.

Figure 7 shows that for all specimens SP-1–6, when the initial diagonal crack occurred, the strain of the flexural reinforcement was 0.33–0.58, which is similar regardless of the specimens, and the average strain was about 0.44. These results indicate that the initial diagonal cracks are generated at the time when the connections undergo a certain amount of flexural damage regardless of the amount of flexural reinforcement or the amount of shear reinforcement of the slab–column connection specimens.

In addition, according to the blue dashed lines in the graphs of SP-2, SP-3, SP-5, and SP-6 which show the ultimate strength and the corresponding displacement of

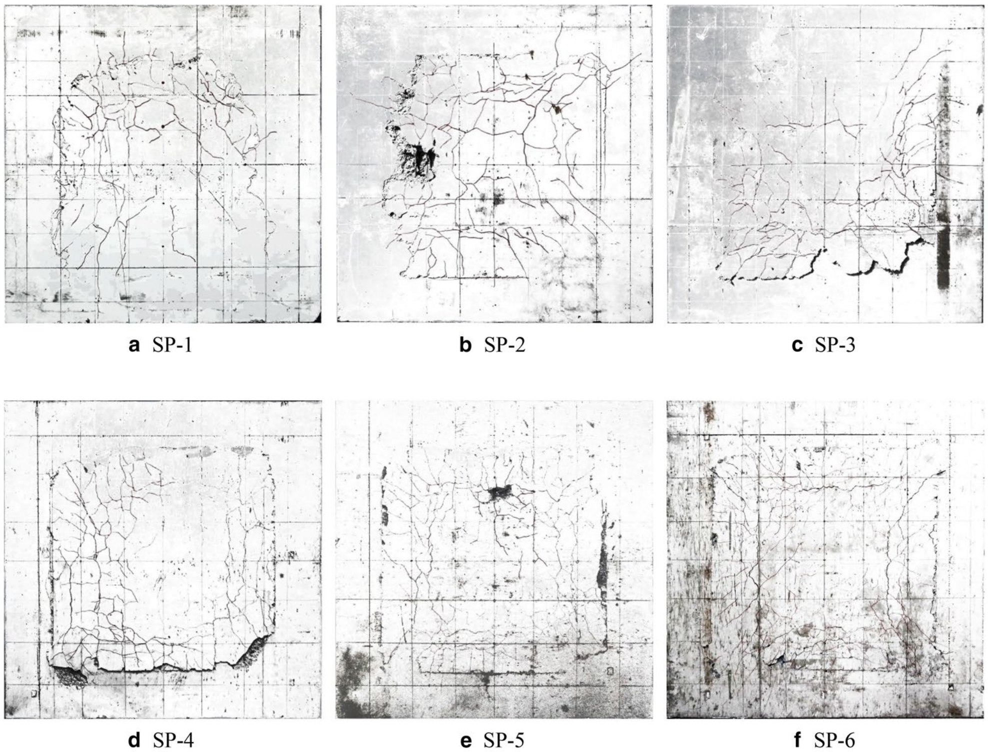

Fig. 5 Concrete cracks at the end of the test.

SP-1 and SP-4 without shear reinforcement, shear reinforcement has little role at the time when the initial diagonal cracking of SP-1 and SP-4 occurred and the concrete resists punching shear.

SP-1–6 were divided into two groups, SP-1–3 and SP-4–6, based on the amount of flexural reinforcement. In the SP-1–3 group, where the amount of flexural reinforcement is small, initial diagonal cracking occurred at a similar center displacement, at 10 mm in all three specimens. According to previous studies (Eom et al. 2018), for specimens whose ultimate strength occurred at the initial diagonal crack, punching shear was resisted mainly by the contribution of the concrete, whereas that of the shear reinforcement to punching shear is not high.

SP-1 (Fig. 7a) without shear reinforcement was damaged by shear without yielding of the flexural rebar; its maximum load is 776 kN. For SP-2 (Fig. 7b) with a low shear reinforcement, the maximum load increased to 1029 kN due to the effect of shear reinforcement, and the strain of the flexural rebar at the diagonal cracking increased. The shear reinforcements yielded at the SA-2 gauge located at the center of the critical section. On the other hand, SP-3 (Fig. 7c), which had more shear reinforcement than SP-2, did not yield for both flexural and shear reinforcements at the maximum load of 970 kN. The strain of shear reinforcement for SP-2 and SP-3 shows a large difference in Fig. 7b, c. As mentioned earlier, shear reinforcements in SP-2 yield, whereas those in SP-3 do not yield. Nevertheless, the ultimate strengths of the two specimens are similar. At similar ultimate loading, the shear reinforcement of SP-3 seems to have a relatively low load resistance, because it had more shear reinforcement than SP-2.

The shear strength of SP-3, in which the flexural reinforcement is relatively small and the shear reinforcement is large, is considered to be limited due to the influence of flexural shear crack behavior (Fig. 8). Figure 8 is a conceptual diagram showing the flexural-shear cracks, whose diagonal shear crack developed from the expansion of initial flexural cracks.

As shown in Fig. 8, if the amount of flexural reinforcement is small and even if the amount of shear reinforcement is large, it is likely that the slab–column connections might fail before the shear reinforcement can sufficiently contribute, because the initial flexural crack developed and the flexural crack width significantly increased. Therefore, shear reinforcement does not play a major role when the amount of flexural reinforcement is small. Consequently, securing only the shear reinforcement at the slab–column connection under a small amount of flexural reinforcement might not be effective to improve the punching shear strength.

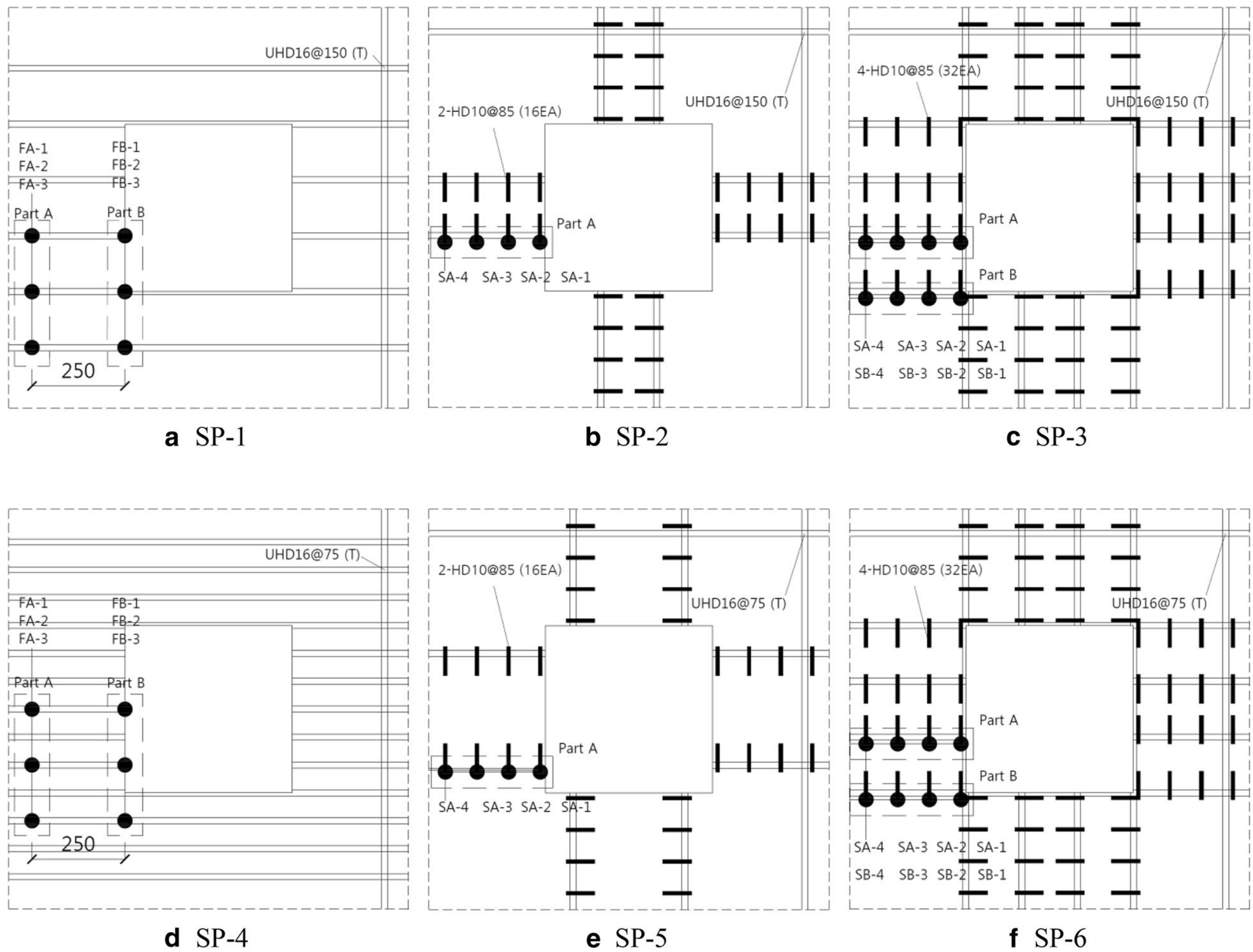

Fig. 6 Setup details of strain gauge.

SP-4 (Fig. 7d) without shear reinforcement failed at a maximum load of 1143 kN and the behavior of the flexural rebar to the maximum load was similar to SP-1. For SP-5 (Fig. 7e) with a low shear reinforcement, the maximum load increased to 1429 kN due to the effect of shear reinforcement, and the strain of the flexural rebar at the diagonal crack increased. Like SP-2, the shear reinforcements yielded at the SA-2 gauge of SP-5 located in the critical section. SP-6 (Fig. 7f), which had more shear reinforcement than SP-5, had 1607 kN load at the initial diagonal crack, which increased gradually to 1713 kN.

In Fig. 7f, the additional strength development phenomenon appears to be caused by the increase in the strength contribution of the shear reinforcement in SP-6 with a large amount of shear reinforcement. However, SP-3, which has the same amount of shear reinforcement, does not behave like SP-6. This difference attributed to the effect of flexural reinforcement, which is the only difference between SP-3 and SP-6. When the amount of flexural reinforcement is large, which controls the expansion of the crack surface and flexure damage after diagonal cracks, the shear reinforcement can play a role properly. In Fig. 7, the strains of the flexural reinforcements after diagonal cracking in SP-4–6 are considerably higher than those in SP-1–3, which also demonstrates the effect of flexural reinforcement. Therefore, in order to improve the punching shear performance of slab–column connections, sufficient flexural reinforcement should be secured, especially when a large amount of shear reinforcement is used.

3.5 Examination and Improvement of Punching Shear Strength Design Formula

Table 5 shows the punching shear strength of SP-1–6 evaluated by test and that predicted by ACI 318 (ACI 2014) and KCI 2012 (KCI 2012) design codes, respectively. Table 5 also shows the ratio of the test results for SP-1–6 to the punching shear strength predictions by ACI 318 (ACI 2014) and KCI 2012 (KCI 2012) design codes. Figure 9 shows the strength ratio as a function

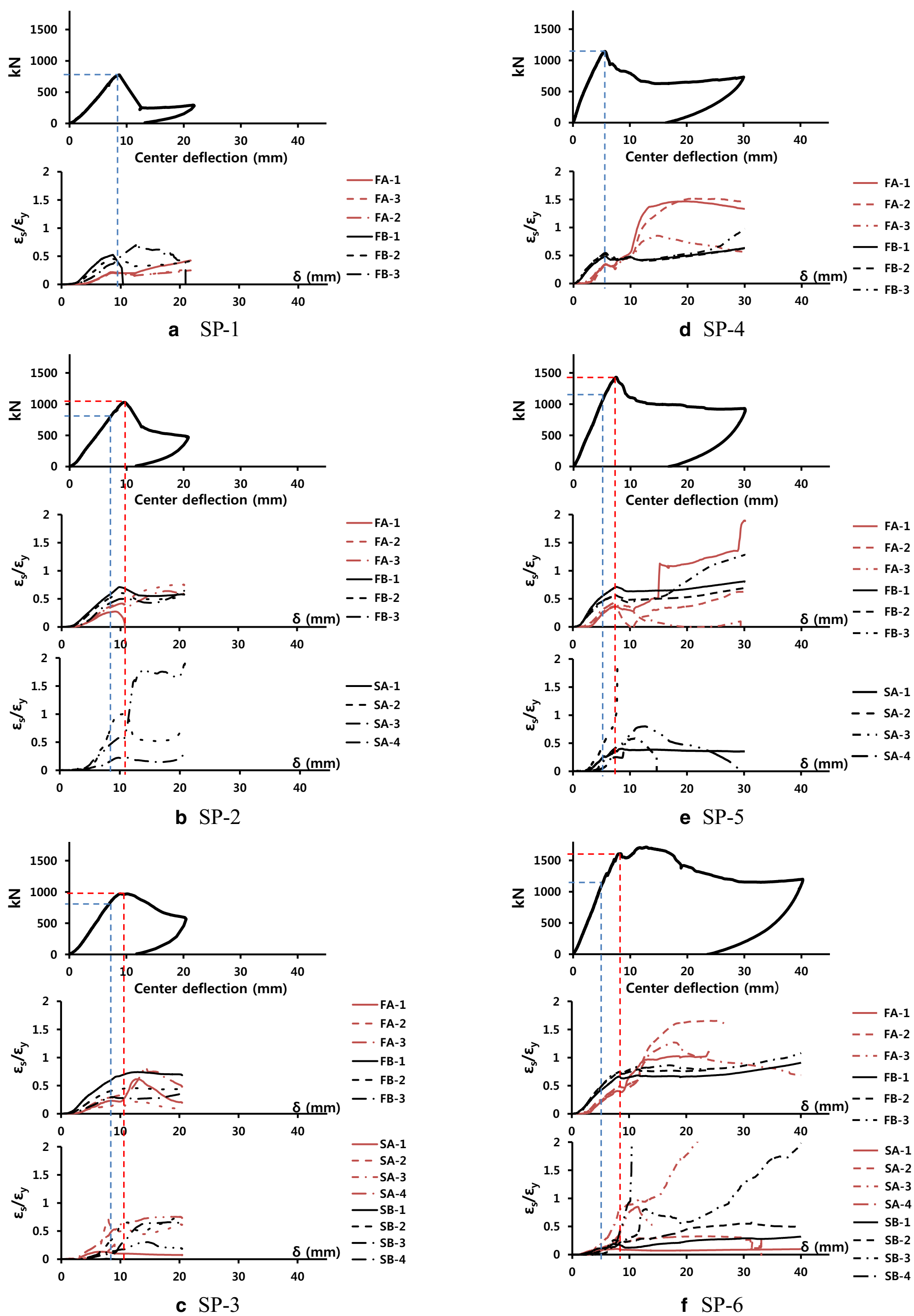

Fig. 7 Strains of flexural and shear reinforcements.

of the amount of shear reinforcement in Table 5. In the graph, the effect of the amount of shear reinforcement with varying the flexural reinforcement ratio and the accuracy of the estimation formula by the codes are shown. Figure 9a, which is based on ACI 318 (ACI 2014), shows a relatively accurate strength estimation when the flexural reinforcement ratio and amount of

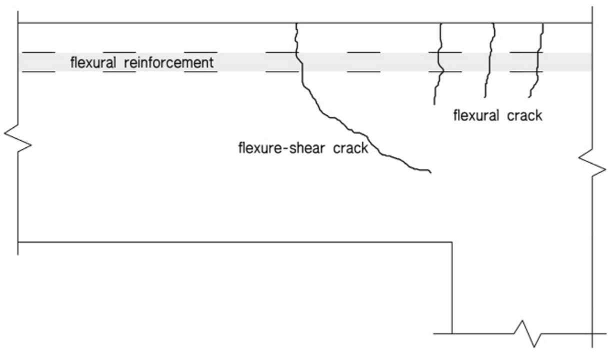

Fig. 8 Diagonal tension crack.

shear reinforcement are small. However, if the amount of shear reinforcement is large while that of the flexural reinforcement is small, the strength of the slab–column connection is overestimated and evaluated as unsafe.

As shown in Fig. 9b, the KCI 2012 (KCI 2012) code accurately estimates the strength of all six specimens, which is possible because the code considers the effect of flexural reinforcement on the punching shear strength by concrete. However, when the flexural reinforcement ratio is low, the strength of the specimen with shear reinforcement is overestimated as the amount of shear reinforcement increases. Therefore, for a specimen with a small amount of flexural reinforcement, it is necessary to add a factor that considers the flexural reinforcement ratio in the calculation of the strength of the shear reinforcement for high accuracy.

A strength reduction factor (α) that can evaluate the performance of the shear reinforcement, which varies with the flexural reinforcement ratio, is proposed in Eqs. (9), (10a) and (10b).

$$V_{n,KCI(modified)} = V_c + 0.5\alpha V_s \tag{9}$$

$$\alpha = 1(\rho \geq 0.014) \tag{10a}$$

$$\alpha = \frac{0.65}{0.007}(\rho - 0.007) + 0.35(0.007 < \rho < 0.014) \tag{10b}$$

where, V_c is the shear strength of the concrete, V_s is the shear strength of the shear reinforcement, α is a strength reduction factor affecting the shear strength of shear reinforcement due to the amount of flexural reinforcement, ρ is the flexural reinforcement ratio.

Equations (9), (10a) and (10b) are design formula that consider the strength reduction of the shear strength by the shear reinforcement based on KCI 2012 (KCI 2012). Table 5 and Fig. 9c show the shear strengths estimated by the above formula and the actual experimental results. Thus, the punching shear strength of the connection with a small amount of flexural reinforcement can be estimated with higher accuracy.

To verify the validity of the proposed method, the proposed method was analyzed using the existing 73 test results by various researchers (Adetta and Polak 2005; Kinnunen and Nylander 1960; Langohr et al. 1976; Mokhtar et al. 1985; Seible et al. 1980; Sherif and Dilger 2000; Vam der Voet et al. 1982; FIP 12. 2001 and etc.) which are same test data analyzed by the previous study (Eom et al. 2018). Detailed specimen properties of the existing test used in this study were introduced in the study by Choi et al. (2011) and Eom et al. (2018). As with the study by Eom et al. (2018), the comparison with tests is limited to the specimens with a total nominal punching shear strength V_n ($=0.5V_c + V_s$) not greater than the allowable maximum by ACI 318 ($=0.5\sqrt{f_c'}\, b_o d$), because specimens with relatively heavy shear reinforcement may be failed by the crushing of concrete strut and therefore the proposed method effectively works for specimens with diagonal shear failure mode. In comparison of the prediction on existing test results by ACI 318 and proposed method, as shown in Fig. 10a, c, the average and COV (coefficient of variation) of V_u/V_n ratios by the proposed method are improved considerably. In comparison of the prediction by KCI 2012 and proposed method, as shown in Fig. 10b, c, the average and COV of V_u/V_n ratios by KCI 2012 and proposed method are almost similar. However, overestimation of punching shear strength

Table 5 Punching shear strength by concrete code.

Specimens	Experiment load (1) (kN)	ACI 318 (2) (kN)	KCI 2012 (3) (kN)	KCI 2012 (4) (modified, kN)	(1)/(2)	(1)/(3)	(1)/(4)
SP-1	776	843.39	752.69	752.69	0.92	1.03	1.03
SP-2	1029	1030.62	1057.19	858	1.0	0.97	1.19
SP-3	970	1639.54	1361.7	962.65	0.59	0.71	1.0
SP-4	1143	949.3	1047.78	1047.78	1.2	1.09	1.09
SP-5	1429	1009.43	1315.16	1316	1.41	1.08	1.08
SP-6	1713	1544.2	1582.56	1583	1.1	1.08	1.08
				Ave	1.037	0.993	1.078
				STDEV	0.277	0.146	0.065

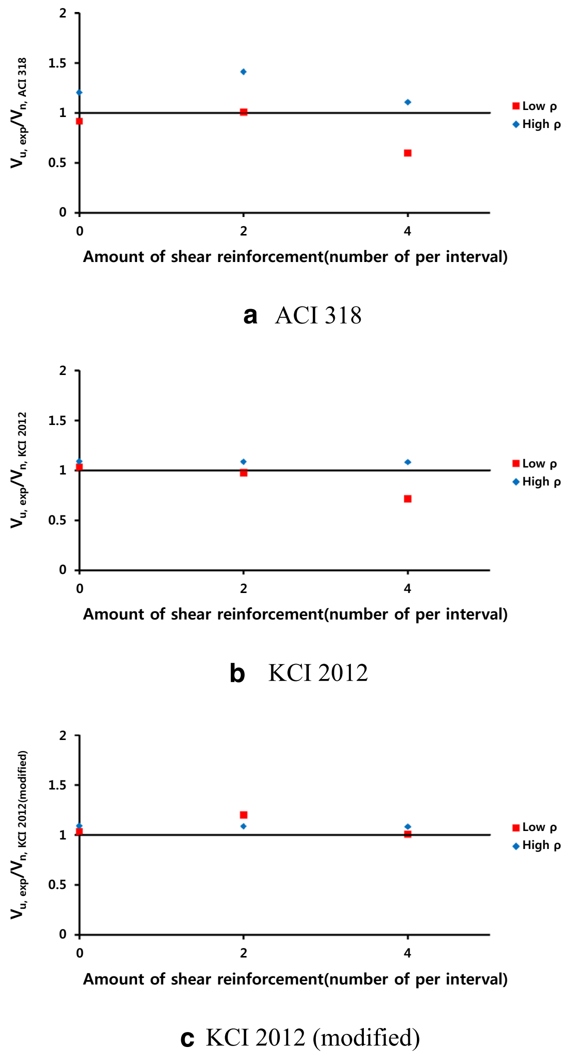

Fig. 9 Comparison of punching shear strengths by concrete code and proposed method.

on the slabs with low flexural reinforcement ratio by KCI 2012 (i.e. $V_u/V_n < 1.0$) was reduced considerably by using the proposed method. Therefore, by using the proposed method, it is possible to perform safe punching shear design for the slabs with low flexural reinforcement ratio.

4 Summary and Conclusions

In this study, to investigate the ultimate punching shear behavior of slab–column connections with varying flexural reinforcement and shear reinforcement, an experimental study was carried out. Six specimens were designed based on the amounts of flexural reinforcement and shear reinforcement. Particularly, the purpose of this study was to verify the effect of flexural reinforcement on the punching shear behavior of shear reinforced slab–column connections. Finally, the current design codes such as ACI 318 (ACI 2014) and KCI 2012 (KCI 2012) were examined to determine whether the effects of various flexural reinforcement ratios on the punching shear strength of shear reinforced slab–column connections are reflected. Finally, a design formula that considers the flexural reinforcement ratio in the calculation of the punching shear strength of the slab–column connection was proposed and verified using experimental results. The primary findings and conclusions of this study are as follows.

1. Due to the punching shear test on the slab–column connection, the amounts of shear reinforcement and flexural reinforcement interactively affect the punching shear strength of the slab–column connection. Specifically, the amount of flexural reinforcement has a significant influence on the behavior of the slab–column connection.
2. Experimental results indicated that the increase of shear reinforcement for a low flexural reinforcement ratio had limitations in increasing the punching shear strength of the connection. When the flexural reinforcement ratio was low, the damage caused by flexure reduces the shear resistance of the shear reinforced slab–column connection.
3. On the other hand, it was confirmed that the shear strength increases with shear reinforcement, when the flexural reinforcement ratio is more than a certain amount. Therefore, when the shear performance of the slab–column connection is insufficient, the amount of flexural reinforcement should be considered rather than simply increasing the amount of shear reinforcement.
4. In a previous study by Eom et al. (2018), if the amount of shear reinforcement was increased regardless of the amount of flexural reinforcement, the ultimate punching strength increased after the initial diagonal crack. However, in this study, the slab–column connection, which had a small amount of flexural reinforcement, behaved differently. Therefore, in itself, the amount of shear reinforcement does not determine this strength increase after initial diagonal cracking, but the flexural reinforcement should be more than a certain amount for this strength increase after initial diagonal cracking.
5. Experimental results evaluated by the KCI 2012 (KCI 2012) design formula and the ACI 318 (ACI 2014) design formula indicate that the punching shear strength evaluation formula of KCI 2012 (KCI 2012), which considers the effect of the flexural reinforcement ratio on the shear strength by concrete is more

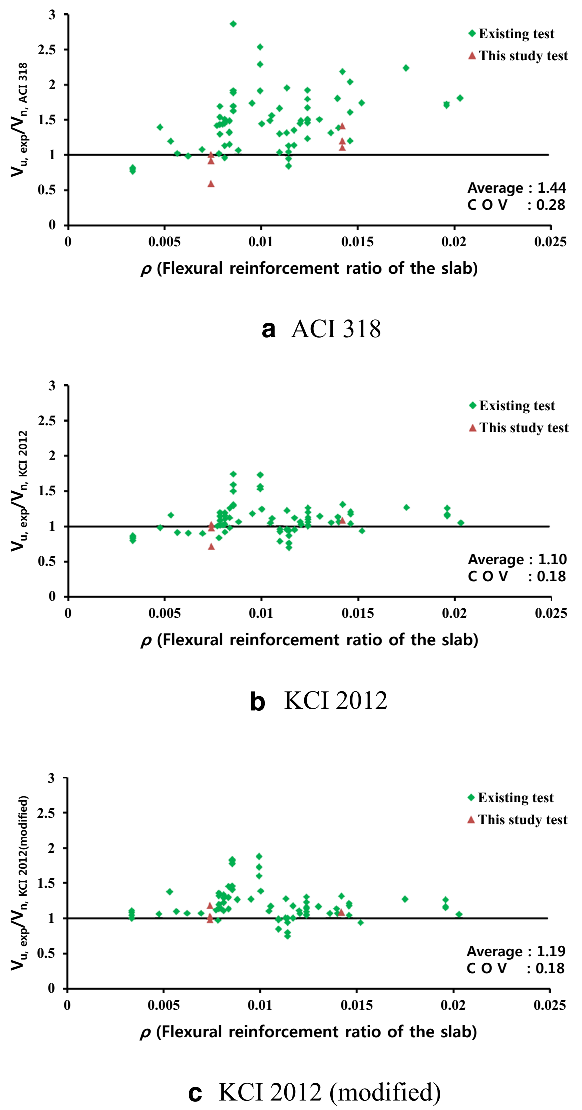

Fig. 10 Comparison of punching shear strengths by concrete code and proposed method (with existing test results).

accurate than that of ACI 318 (ACI 2014). However, in both design formula, shear strength evaluation for the shear reinforcement tends to overestimate the shear strength when the flexural reinforcement ratio is low and the amount of shear reinforcement is large, as the effect of flexural reinforcement on the shear strength, by the amount of shear reinforcement, is not considered.

6. Thus, the strength reduction factor for the shear reinforcement considering the effect of flexural reinforcement was proposed. Using the proposed method, the punching shear strength of shear reinforced slab–column connection could be estimated more stably. And the validity of the proposed strength reduction factor was verified by comparing its prediction results with existing test data.

The proposed method in this study is limited to concentric axial loading to the slabs with symmetric longitudinal bar condition. Therefore, further study is needed to analyze the punching shear strength of the slabs with asymmetric longitudinal bars under various loading conditions such as eccentric or lateral loadings.

Authors' contributions

JIJ performed the experiments. Also, JIJ analyzed the data and wrote the paper. SMK planed this study, reviewed all the data analyzed and the paper written by JIJ, and supervised this project. Both authors read and approved the final manuscript.

Acknowledgements

This work was supported by the National Research Foundation of Korea (NRF) grant funded by the Korea government (MSIP) (No. 2015R1C1A1A01053471). And this research was financially supported by the National Research Foundation of Korea (NRF) grant funded by the Korea government (MSIT) (No. 2018R1A2B6007559).

Competing interests

The authors declare that they have no competing interests.

Availability of data and materials

All data analyzed during this study are available in the master's course thesis of J. I. Jang at Chungbuk National University in 2019.

Publisher's Note

Springer Nature remains neutral with regard to jurisdictional claims in published maps and institutional affiliations.

Received: 27 November 2018 Accepted: 11 March 2019
Published online: 01 May 2019

References

ACI Committee 318. (2014). *Building code requirements for structural concrete (ACI 318-14) and commentary*. Farmington Hills: American Concrete Institute.

Adetta, B., & Polak, M. A. (2005). Retrofit of slab column interior connections using shear bolts. *ACI Structural Journal, 102*(2), 268–274.

Choi, M. S., Ahn, J. M., Lee, K. S., & Shin, S. W. (2005). Influence of column aspect ratio on the punching shear strength of interior flat plate slab–column connections. *Journal of the Architectural Institute of Korea, 21*(10), 79–86.

Choi, C. S., Bae, B. I., Choi, Y. C., & Choi, H. K. (2012). The effect of anchorage with shear reinforcement in flat plate system. *Journal of the Korea concrete Institute, 24*(6), 667–675.

Choi, K. K., Kim, S. H., Kim, D. H., & Park, H. G. (2011). Direct punching shear strength model for interior slab–column connections and column footings with shear reinforcement. *Journal of the Korea concrete Institute, 23*(2), 159–168.

Choi, K. K., & Park, H. G. (2010). Shear strength model for interior flat plate–column connection. *Journal of the Korea concrete Institute, 22*(3), 345–356.

Choi, J. W., & Song, J. K. (2007). The punching shear strength of lightly reinforced thick flat plates without shear reinforcement. *Journal of the Architectural Institute of Korea, 23*(8), 67–74.

Eom, T. S., Kang, S. M., Choi, T. W., & Park, H. K. (2018). Punching shear tests of slabs with high-strength continuous hoop reinforcement. *ACI Structural Journal, 115*(5), 1295–1305.

FIP 12. (2001). *Punching of structural concrete slabs*. Lausanne: CEB-FIP Task Group.

Kinnunen, S., & Nylander, H. (1960). Punching of concrete slabs without shear reinforcement. *Royal Institute of Technology, Stockholm, 158,* 112.
Korean Concrete Institute. (2012). *Concrete structure design code (KCI 2012)*. Seoul: Korean Concrete Institute.
Langohr, P. H., Ghali, A., & Dilger, W. H. (1976). Special shear reinforcement for concrete flat plates. *ACI Structural Journal, 73*(3), 141–146.
Mokhtar, A., Ghali, A., & Dilger, W. H. (1985). Stud shear reinforcement for flat concrete plates. *ACI Structural Journal, 82*(5), 676–683.
Seible, F., Ghali, A., & Dilger, W. H. (1980). Preassembled shear reinforcing units for flat plates. *ACI Structural Journal, 77*(1), 28–35.
Sherif, A. G., & Dilger, W. H. (2000). Tests of full-scale continuous reinforced concrete flat slabs. *ACI Structural Journal, 97*(3), 455–467.
Vam der Voet, A. F., Dilger, W. H., & Ghali, A. (1982). Concrete flat plates with well-anchored shear reinforcement elements. *Canadian Journal of Civil Engineering, 9*(1), 107–114.